CMTM6 maintains B cell-intrinsic CD40 expression to regulate anti-tumor immunity

Authors: Yiru Long[1,2], Runqiu Chen[3,1], Wenlong Chang[4,1], Hanyue Luo[4,1], Fanglin Li[1,2], Jianhua Sun[1,5], Jing Chen[1,2], Likun Gong[1,2,4,5*]

Affiliations:

[1]State Key Laboratory of Drug Research, Shanghai Institute of Materia Medica, Chinese Academy of Sciences, Shanghai, China

[2]University of Chinese Academy of Sciences, Beijing, China

[3]Department of Microbiological and Biochemical Pharmacy, School of Pharmacy, Fudan University, Shanghai, China

[4]School of Public Health, China Medical University, Shenyang, China

[5]Zhongshan Institute for Drug Discovery, Shanghai Institute of Materia Medica, Chinese Academy of Sciences, Zhongshan, China.

*Correspondence: Likun Gong (lkgong@simm.ac.cn)

Running title: The CMTM6-CD40 axis in B cell anti-tumor immunity

Highlights

- B cells participate in anti-tumor immunity by influencing the intratumoral infiltration and function of T cells;
- CMTM6 cis-interacts with CD40 to maintain CD40 cell membrane levels;
- Loss of B cell-intrinsic CMTM6 significantly reduces CD40 signaling-mediated B cell activation, survival, and differentiation;
- CMTM6 deficiency leads to a significant reduction in the anti-tumor activity of B cells and CD40 agonists.

In Brief

Long et al. demonstrate that B-cell intrinsic CMTM6 regulates CD40 signaling and function via maintaining the cell membrane level of B-cell CD40 through a post-translational modification pathway, thereby affecting anti-tumor B-cell immunity and the efficacy of CD40 agonist.

SUMMARY

Tumor cell CMTM6 is a novel tumor immunoregulator involved in maintaining membrane levels of several important molecules, such as PD-L1 and CD58. Host CMTM6 may also play a function in the tumor microenvironment. Here, we found that CMTM6 was highly expressed in splenic B cells and tumor-infiltrating B cells. CMTM6 deficiency resulted in impaired splenic development, germinal center B cell differentiation, memory B cell differentiation, and B cell anti-tumor immune responses. Through multi-omics data mining and B-cell agonist screening, we identified that CMTM6 interacted with CD40 and maintained CD40 membrane levels in B cells. CMTM6 regulated CD40 at the post-translational modification stage but not at the transcriptional stage. CMTM6 deficiency led to impaired CD40 signaling-mediated B cell activation, survival, proliferation, and differentiation. In vivo, CMTM6 deficiency leads to a significant decrease in the anti-tumor activity of B cell-dependent CD40 agonists. Collectively, B-cell intrinsic CMTM6 maintains B cell CD40 levels and signaling to promote B cell function and anti-tumor immunity.

INTRODUCTION

T cells are absolutely central to tumor immunotherapy as represented by immune checkpoint blockade (ICB) therapies, and the primary objective of these therapies is to restore or improve T cell anti-tumor activity. However, the complex composition of the tumor microenvironment (TME), as well as the current status of disappointing treatment response rates, indicate that focusing solely on T cells is inadequate[1]. T and B cells are crucial to adaptive immune responses, but the importance of B cell in antitumor immunity remains unappreciated. While B cells can eliminate tumor cells through tumor-targeting antibodies that facilitate antibody-dependent cellular cytotoxicity (ADCC) and antibody-dependent cellular phagocytosis (ADCP), previous research has mostly concentrated on the tumor-promoting impacts of B cells[2]. Studies on the critical role tumor infiltrating B-lymphocytes (TIL-B) play in the ICB response and antitumor effects have emerged in recent years. The development of intratumoral tertiary lymphoid structures (TLS) relies on TIL-B cells, which are essential for the acquisition and presentation of tumor antigens, as well as for the promotion of tumor-specific T follicular helper cells (Tfh) differentiation and anti-tumor $CD8^+$ T-cell activation[3,4]. Patients with early-stage lung adenocarcinoma, melanoma, sarcoma, or renal cell carcinoma exhibit a positive correlation between B-cells/TLS and their response to cancer immunotherapy[5-8]. Besides, molecules like TIM-1 have been discovered to regulate B-cell responses to tumors, indicating potential therapeutic approaches for targeting TIL-B[9,10].

CKLF-like MARVEL transmembrane domain-containing protein 6 (CMTM6), identified in 2003, is an M-shaped four-transmembrane protein[11]. CMTM6 has been reported to be associated with the prognosis and advancement of various clinical malignancies, and it is thought to affect tumor progression via several possible pathways, such as the WNT pathway[12-15]. In recent years, tumor cell intrinsic CMTM6 has been discovered as a novel tumor immunoregulatory protein. CMTM6 is a new post-translational modification regulatory molecule of PD-L1, capable of inhibiting the endosomal-lysosomal and ubiquitin-proteasomal degradation pathways of PD-L1, extending the half-life of tumoral PD-L1, and modulating tumor immunity[16,17]. CMTM6 has also been shown to prevent the lysosomal degradation of CD58 in tumor cells, modulating the anti-tumor responses of T cells[18,19]. Our previous studies revealed that tumor cell CMTM6 could

regulate $CD8^+$ T cell anti-tumor immunity by maintaining PD-L1 bidirectional signaling and PD-L1-independent β-catenin/CCL4 signaling[20,21]. We also developed two drug candidates, CMTM6-targeted nanobodies and adeno-associated viruses, and confirmed their significant antitumor activity in vivo[20,21]. However, the expression and function of CMTM6 in tumor-infiltrating immune cells have not been systematically studied.

In this study, we investigated the anti-tumor immune role of B cells with an eye on CMTM6, and systematically elucidated the expression of CMTM6 in B cells as well as the regulatory roles and mechanisms of CMTM6 on B cell function and anti-tumor immunity.

RESULTS

B cells influence the TME and anti-tumor T cell responses

We initially examined the impact of total B lymphocytes on tumor immunity. We used the anti-CD20 antibody to delete B cells in tumor-bearing mice and confirmed the effect in draining lymph nodes (dLN) and tumors at the anatomical endpoint (Figures S1A and S1B). In the B16F10 tumor model, we discovered that in the absence of B cells, the leukocytes infiltrating the tumor were dramatically reduced, particularly $CD4^+$ and $CD8^+$ T cells, to roughly 15% of their original levels (Figure S1C). Similarly, in the MC38 tumor model, B-cell deletion also interfered with intratumoral infiltration of leukocytes and T cells (Figure S1E). Moreover, in the draining lymph nodes, the expression of T-cell effector molecules, such as interferon-γ (IFN-γ), granzyme B (GzmB), and perforin, was impaired after B-cell deletion (Figures S1D and S1E). These findings, once again, point to the fact that total B cells generally have antitumor effects and can encourage T cell infiltration and function within tumors.

CMTM6 is expressed in peripheral and tumor B cells

Using open-source single-cell sequencing data, we determined that CMTM6 was more abundantly expressed on B cells in the peripheral blood of humans or mice (Figure S2A). CMTM6 was similarly extremely expressed in B cells that infiltrated the tumor (Figure S2B). We also confirmed the higher levels of CMTM6 in mouse splenic B cells via flow cytometry (Figure S2C). On the basis of these results, we hypothesized that CMTM6 serves an essential role in B cells.

CMTM6 is a potential regulator of B-cell anti-tumor immunity

We then proceeded to compare the effects of CMTM6 knockout (KO) on the antitumor activity of B cells. When comparing the differences in immune organs between wild-type (WT) and *Cmtm6* KO mice, we found that the spleen size differed significantly between the two, with CMTM6 defects resulting in mice with smaller spleens and significantly lower spleen indexes (Figure 1A). In the MC38-OVA and B16-OVA subcutaneous tumor models, the spleens of *Cmtm6* KO mice also were smaller (Figure 1B). Considering that B cells are the predominant cell type in the spleen, we hypothesized that CMTM6 may affect B cell development, proliferation, or survival.

To investigate whether CMTM6 affects certain biological processes in B cells, we first performed RNA sequencing (RNA-seq) analysis on spleen tissues of WT and *Cmtm6* KO mice, and the results showed that the differential genes were indeed enriched in several pathways related to B cell, such as "positive regulation of B cell activation" (Figure 1C). Further, we

isolated splenic B cells from WT and *Cmtm6* KO mice by magnetic cell sorting, followed by RNA-seq analysis, which showed enrichment of differential genes into immune and cancer-related pathways (Figure 1D). These results once again suggest a correlation between CMTM6 and B cell function.

In vivo, we eliminated B cells using the anti-CD20 antibody and discovered that B cell deletion resulted in faster B16F10 tumor growth in WT mice, implying that total B cells have anti-tumor effects (Figure 1E). In *Cmtm6* KO mice, the deletion of B cells further impeded tumor progression in vivo, indicating that CMTM6-deficient B cells have impaired anti-tumor activity (Figure 1E). To facilitate a more precise comparison of the antitumor effects of WT B cells and CMTM6-deficient B cells, we infused them peritumorally into mice with original B cell deletion (Figure S3A). The results indicated that, in the MC38 or B16F10 tumor model, tumor progression was inhibited by the infiltration of WT B cells with inhibition rates (IR) of 60.6% and 37.1% separately, whereas the infiltration of CMTM6-deficient B cells did not achieve noticeable antitumor effects (Figures 1F and 1G). Furthermore, the efficacy of CMTM6-deficient B cells in promoting T-cell responses was also compromised in the dLN of B16F10 tumors (Figure S3B). Taken together, these findings suggest that CMTM6 may be associated with B cell function and involved in maintaining the anti-tumor immune response of B cells.

CMTM6 affects B cell differentiation

Next, we planned to systematically investigate the regulatory role of CMTM6 on B cells. Our initial emphasis was on the impact of CMTM6 on B cell differentiation. We used flow cytometry to compare the percentages of each subpopulation of splenic B cells in WT and *Cmtm6* KO mice (Figure S4). We discovered that CMTM6 deficiencies had no significant effect on the proportion of total splenic B cells, as well as the percentages of B1 cells, B2 cells, marginal zone B cells, follicular B cells, immature B cells, mature B cells, and plasma cells (Figures S5A-D).

Notably, CMTM6-deficient mice showed considerably decreased percentages of splenic non-class-switching memory B cells, class-switching memory B cells, and germinal center B cells (Figures 2A and 2B). In mouse lymph nodes, the percentage of lymph node memory B cells and germinal center B cells was also much lower in CMTM6-deficient mice (Figures 2C and 2D). Moreover, by comparing splenic B cell subpopulations in *Cd274* KO mice and *Cmtm6*/*Cd274* double-KO mice, it was found that, in the absence of the PD-L1 axis, CMTM6 defects still resulted in a reduction of memory B cells and germinal center B cells (Figures 2E and 2F). These findings demonstrate that CMTM6 deficiency impairs B cell differentiation or survival to memory B cells and germinal center B cells, independently of PD-L1. CMTM6 may have impacted critical molecules in this biological process. Since mice do not express CD58, we left aside the question of whether CD58 plays a role.

CMTM6 affects CD40-mediated B cell activation

To investigate the effect of CMTM6 on B cell immune function, we used five commonly used B cell agonists to compare the activation status of wild-type B cells and CMTM6-deficient B cells: the TLR4 agonist LPS, the TLR7 agonist Imiquimod, the TLR9 agonist Agatolimod, the BCR agonist anti-IgM antibody, and the CD40 agonist FGK45 antibody. Statistical analysis showed that B cell activation levels were similar between WT and *Cmtm6* KO splenocytes following TLR4, TLR7, TLR9, and BCR activation (Figures S6A-D), but differed considerably after anti-CD40 stimulation (Figures 3A-C). Specifically, B cells in the CMTM6-deficient splenocytes expressed considerably lower amounts of CD69, CD86, and major histocompatibility complex

class II (MHC II) than those in the WT group, indicating decreased activation (Figures 3A-C). To exclude out the interference of other immune cells in the splenocytes, we analyzed the activation of sorted B cells. We discovered that CMTM6-deficient B cells also exhibited significantly lower CD86 and MHC II expression compared to WT B cells when exposed to CD40 agonists (Figure 3D and 3E). Interestingly, there was no discernible increase in activation, even when compared to vehicle controls (Figure 3D and 3E). Clustering of CMTM6-deficient B was also notably decreased after FGK45 action (Figure S7). In addition, we arrived at the same conclusion after comparing the variations in lymph node B cells between WT and *Cmtm6* KO mice subsequent to anti-CD40 antibody activation (Figures 3F-H). These findings imply that CMTM6 does have an effect on B cell immunological function, and that the CD40 pathway may be a possible mechanism for CMTM6 regulating B cell immunity.

CMTM6 maintains membrane levels of CD40 in B cells

Given the studies that have shown that CMTM6 interacts with two single-transmembrane proteins, PD-L1 and CD58, we speculated that CMTM6 may also interact with CD40, which is also a single-transmembrane receptor. Subsequently, by mining publicly available protein interactions data, we found that potential interactions between CMTM6 and CD40 were seen in yeast two-hybrid libraries, affinity-purified proteomics, and membrane proteomics of CMTM6 knockouts (Figure S8A). In addition, in open-source CRISPR screening data, we also found that KO of CMTM6 in human B-cell lymphoma cells Daudi affected the membrane level of CD40 (Figure S8B).

Therefore, we postulated that CMTM6 may also affect membrane levels of CD40 in B cells. Our findings indicate that, in comparison to WT mice, CMTM6 deficiency considerably decreased membrane CD40 in total splenic B cells and significantly decreased membranal CD40 in immature, mature, naïve, memory, and germinal center B cells (Figures 4A and 4B). In mouse lymph nodes, CMTM6 deficiencies also caused downregulation of CD40 membrane levels in broad B cell subsets (Figure 4C). We compared B-cell CD40 expression in *Cmtm6*/*Cd274* double-KO mice and *Cd274* KO mice to confirm the function of the PD-L1 axis in regulating CD40 membrane levels by CMTM6 (Figure 4D). Our findings revealed that CMTM6 defects similarly decreased membranal CD40 in the absence of the PD-L1 axis (Figure 4D). Besides, ablation of CMTM6 also reduced CD40 membrane levels in splenic B cells in MC38-OVA or B16-OVA tumor-bearing mice (Figure 4E). These findings show that CMTM6 is a regulatory molecule for B cell CD40 independently of PD-L1.

CMTM6 maintains function of CD40 in B cells

We therefore postulated that CMTM6 may influence CD40 downstream signaling and function through regulating its membrane levels. We sorted primary splenic B cells from WT and *Cmtm6* KO mice and acted on them with CD40 agonist for 15 min, respectively. Phospho flow cytometry revealed that CMTM6-deficient B cells had significantly reduced levels of phosphorylated p65 and p38, suggesting that CMTM6 indeed affects CD40 signaling in B cells (Figures 4F and 4G).

During in vitro culture, primary B cells quickly undergo an apoptotic process, and CD40 signaling can increase anti-apoptotic and proliferation of B cells. B cells from WT mice showed increased survival after 72 hours of CD40 agonist treatment due to a dose-dependent anti-apoptotic effect, which was not observed in the CMTM6 deficiency group (Figure 4H). CD40 agonist-induced B cell proliferation was also strongly influenced by CMTM6 KO in CCK8

assays (Figure 4I). CD40 signaling can enhance the development of germinal center B cells. We observed a dose-dependent differentiation of WT B cells into $GL7^+$ $CD95^+$ germinal center B cells when treating primary B cells in vitro with CD40 agonists (Figure 4J). However, the differentiation of B cells was notably decreased in CMTM6 KO mice (Figure 4J).

Collectively, CMTM6 affects CD40 signaling-mediated B cell activation, proliferation, survival, and differentiation through its effect on B cell CD40 membrane levels.

CMTM6 is an interacting molecule of CD40

The foregoing findings suggest that CMTM6 is a new regulatory molecule for B cell immunity, and that the CMTM6-CD40 axis controls B cell function. Therefore, we aim to investigate the mode of CMTM6-CD40 interaction in depth. We then pulled CD40 protein based on the anti-CMTM6 antibody in human B-cell lymphoma cell line Raji samples and mouse splenocyte samples by Co-IP assay, and the results showed that CMTM6 and CD40 did have direct interaction (Figures 5A and 5B). AlphaFold2 was utilized to predict the structures of human and mouse CMTM6/CD40 complexes, human and mouse CMTM6/PD-L1 complexes, and human CMTM6/CD58 complexes (Figure 5C). The interaction interfaces within these complexes were also analyzed (Figure 5D). The sites of interaction in CMTM6 were highly similar between CD40/CD58/PD-L1, and the main regions of interaction were located in the first transmembrane domain, the second transmembrane domain, and the first extracellular domain of the CMTM6 protein. The sites of interaction on CD40 were mainly located in the transmembrane domain and the proximal transmembrane region.

B-cell CMTM6 impacts the antitumor efficacy of CD40 agonists

The above results illustrate that CMTM6 affects B-cell immunity by interacting with CD40 and maintaining B-cell CD40 membrane levels and regulating CD40 signaling and function. In the B16F10 subcutaneous tumor model, we discovered that CD20 antibody-mediated deletion of B cells in mice significantly affected the antitumor activity of CD40 agonists (Figure 6A), and similar phenomena were observed in the CT26 and MC38 models (Figures 6B and 6C), implying that B cells are one of the pharmacological target cells for CD40 agonists. Next, in the B16F10 model and MC38 model, we found that KO of host CMTM6 significantly reduced the in vivo antitumor activity of CD40 agonists (Figures 6D and 6E). Considering our findings that CMTM6 regulates B-cell CD40 and B-cell immunity, we hypothesized that CMTM6 may influence the antitumor efficacy of CD40 agonists by regulating CD40 signaling in B cells. This speculation will be validated in subsequent experiments with B-cell CMTM6 conditional KO mice.

DISCUSSION

In this work, we investigated the influence of the CMTM6-CD40 axis in B cell differentiation, B cell immunity and B cell anti-tumor immune effects.

In previous studies, B cells have often been considered to be bystanders to tumor immunity or to have pro-tumorigenic effects. Initially, researchers discovered that the anti-tumor effects of T cells were boosted in the B-cell-deficient mice μMT[22,23]. The researchers also identified a subpopulation of B cells with immunosuppressive functions called regulatory B cells (Bregs)[24]. Bregs, which expresses IL-10 as a marker, can suppress anti-tumor immunity by secreting IL-10, IL-35, TGF-β, IL-1β, or expressing checkpoint molecules such as PD-1 and PD-L1[25-27]. In addition, IgA antibodies produced by B cells have also been reported to dampen the cytotoxicity of $CD8^+$ T cells[28]. But as we mentioned earlier, the antitumor role of B cells has received more

attention in recent years. Moreover, the latest researches have raised questions about the role of tumor-promoting factors produced by B cells. The researchers found that conditional KO of IL-10 in B cells did not inhibit tumor growth[9]. IgA antibodies have also been reported to enter tumor cells via transcytosis, block oncogenic signals, and promote T cell-mediated cytotoxicity[29]. Our findings reaffirm that total B cells possess anti-tumor effects and can promote intratumor T cell infiltration and effects. We also discovered that CD40 agonists rely on B cells for effectiveness, indicating that B cells may play a crucial role in tumor immunotherapy. Of course, further investigation is required to understand the role and function of B lymphocytes in the tumor microenvironment in order to maximize their potential in tumor immunotherapy.

We identified CMTM6 as a novel regulatory molecule of B cell intrinsic CD40. CD40 signaling is crucial for B cell proliferation, survival, activation, differentiation, and antibody production[30]. By modulating CD40 signaling, CMTM6 was involved in B cell survival, activation, differentiation, proliferation, and antitumor immunity. In line with findings reported in previous research involving *Cd40* KO mice or *Cd40l* KO mice[31,32], *Cmtm6* KO mice displayed atypical quantities of germinal center B cells and memory B cells. In recent years, several studies have also validated that strong CD40/CD40L interactions are critical for B cell differentiation[33,34]. Interestingly, although KO of CMTM6 resulted in only about a 30% decrease in CD40 membrane levels, CD40 signaling and function were significantly attenuated. Our hypothesis posits that CMTM6, apart from its role in CD40 membrane level regulation, might also participate in the interplay of signals between CD40L and CD40 as a component of the CD40 signaling complex.

Our results suggest that CMTM6 is a novel interacting molecule of CD40. Recent studies have identified CMTM6 as a molecule that interacts with numerous transmembrane proteins, including PD-L1, CD58, and HER2[16-19,35]. CMTM6 regulates the membrane levels of these proteins in the post-translational modification pathway, impacting tumor growth and tumor immunity. Considering the predicted structure of CMTM6 and the similar interaction patterns of CMTM6 with other proteins, we hypothesize that CMTM6 might serve as a chaperone protein responsible for sustaining the stability of various transmembrane proteins. Interestingly, molecules regulated by CMTM6 exhibit variable functions in the progression of tumors, indicating the intricate function of CMTM6 in the tumor microenvironment.

In summary, our work demonstrates that B-cell intrinsic CMTM6 regulates CD40 signaling and function via maintaining the B-cell membranal CD40 through a post-translational modification pathway, thereby affecting B-cell differentiation and function, anti-tumor B-cell immunity, and the efficacy of CD40 agonists. These studies will broaden the knowledge of the anti-tumor effects of B cells and the regulatory mechanism for CD40, elucidate the role and mechanism of CMTM6 in the TME, and inspire the value of B cell CMTM6 for potential clinical applications.

Limitations of the study

In the present study, we did not validate the regulatory effect of CMTM6 on B-cell antitumor immunity in an in-situ tumor model and an immune-humanized tumor model due to the limitation of conditions. Besides, considering that CMTM6 and CD40 are also highly expressed in macrophages, neutrophils, etc., we should also explore the role of the CMTM6-CD40 axis in other immune cells in future studies.

SUPPLEMENTAL INFORMATION

Figures. S1 to S8

ACKNOWLEDGMENTS

This work was supported by the China Postdoctoral Science Foundation (2023M743659 and 2023TQ0364), the Shanghai Post-doctoral Excellence Program (2023699), and the Postdoctoral Fellowship Program of CPSF (GZB20230797). All the schematics are were created with BioRender.com.

AUTHOR CONTRIBUTIONS

Conceptualization, L.G. and Y.L.; Methodology, Y.L. and R.C.; Formal Analysis, Y.L.; Investigation, Y.L., R.C, W.C., H.L., and F.L.; Resources, L.G., J.C., J.S., Y.L.; Writing – Original Draft, Y.L.; Writing – Review & Editing, L.G. and Y.L.; Supervision, L.G.; Funding Acquisition, L.G. and Y.L.

DECLARATION OF INTERESTS

The authors declare that they have no competing interests.

REFERENCES

1. Binnewies, M., Roberts, E.W., Kersten, K., Chan, V., Fearon, D.F., Merad, M., Coussens, L.M., Gabrilovich, D.I., Ostrand-Rosenberg, S., Hedrick, C.C., et al. (2018). Understanding the tumor immune microenvironment (TIME) for effective therapy. Nat. Med. *24*, 541-550. 10.1038/s41591-018-0014-x.
2. Downs-Canner, S.M., Meier, J., Vincent, B.G., and Serody, J.S. (2022). B Cell Function in the Tumor Microenvironment. Annu Rev Immunol *40*, 169-193. 10.1146/annurev-immunol-101220-015603.
3. DiLillo, D.J., Yanaba, K., and Tedder, T.F. (2010). B cells are required for optimal CD4+ and CD8+ T cell tumor immunity: therapeutic B cell depletion enhances B16 melanoma growth in mice. J Immunol *184*, 4006-4016. 10.4049/jimmunol.0903009.
4. Cui, C., Wang, J., Fagerberg, E., Chen, P.M., Connolly, K.A., Damo, M., Cheung, J.F., Mao, T., Askari, A.S., Chen, S., et al. (2021). Neoantigen-driven B cell and CD4 T follicular helper cell collaboration promotes anti-tumor CD8 T cell responses. Cell *184*, 6101-6118 e6113. 10.1016/j.cell.2021.11.007.
5. Cabrita, R., Lauss, M., Sanna, A., Donia, M., Skaarup Larsen, M., Mitra, S., Johansson, I., Phung, B., Harbst, K., Vallon-Christersson, J., et al. (2020). Tertiary lymphoid structures improve immunotherapy and survival in melanoma. Nature *577*, 561-565. 10.1038/s41586-019-1914-8.
6. Helmink, B.A., Reddy, S.M., Gao, J., Zhang, S., Basar, R., Thakur, R., Yizhak, K., Sade-Feldman, M., Blando, J., Han, G., et al. (2020). B cells and tertiary lymphoid structures promote immunotherapy response. Nature *577*, 549-555. 10.1038/s41586-019-1922-8.
7. Petitprez, F., de Reynies, A., Keung, E.Z., Chen, T.W., Sun, C.M., Calderaro, J., Jeng, Y.M., Hsiao, L.P., Lacroix, L., Bougouin, A., et al. (2020). B cells are associated with survival and immunotherapy response in sarcoma. Nature *577*, 556-560. 10.1038/s41586-019-1906-8.
8. Hao, D., Han, G., Sinjab, A., Gomez-Bolanos, L.I., Lazcano, R., Serrano, A., Hernandez, S.D., Dai, E., Cao, X., Hu, J., et al. (2022). The Single-Cell Immunogenomic Landscape of B and Plasma Cells in Early-Stage Lung Adenocarcinoma. Cancer Discov. *12*, 2626-2645. 10.1158/2159-8290.CD-21-1658.

9. Bod, L., Kye, Y.C., Shi, J., Torlai Triglia, E., Schnell, A., Fessler, J., Ostrowski, S.M., Von-Franque, M.Y., Kuchroo, J.R., Barilla, R.M., et al. (2023). B-cell-specific checkpoint molecules that regulate anti-tumour immunity. Nature *619*, 348–356. 10.1038/s41586-023-06231-0.
10. Zhang, Z., Xu, X., Zhang, D., Zhao, S., Wang, C., Zhang, G., Chen, W., Liu, J., Gong, H., Rixiati, Y., et al. (2024). Targeting Erbin-mitochondria axis in platelets/megakaryocytes promotes B cell-mediated antitumor immunity. Cell Metab. 10.1016/j.cmet.2023.12.020.
11. Han, W., Ding, P., Xu, M., Wang, L., Rui, M., Shi, S., Liu, Y., Zheng, Y., Chen, Y., Yang, T., and Ma, D. (2003). Identification of eight genes encoding chemokine-like factor superfamily members 1–8 (CKLFSF1–8) by in silico cloning and experimental validation. Genomics *81*, 609-617. 10.1016/s0888-7543(03)00095-8.
12. Liang, J., Li, S., Li, W., Rao, W., Xu, S., Meng, H., Zhu, F., Zhai, D., Cui, M., Xu, D., et al. (2022). CMTM6, a potential immunotherapy target. J. Cancer Res. Clin. Oncol. *148*, 47-56. 10.1007/s00432-021-03835-9.
13. Yaseen, M.M., Abuharfeil, N.M., and Darmani, H. (2022). CMTM6 as a master regulator of PD-L1. Cancer Immunol. Immunother. 10.1007/s00262-022-03171-y.
14. Liu, Q., Wang, J., Guo, Z., Zhang, H., Zhou, Y., Wang, P., Li, T., Lu, W., Liu, F., and Han, W. (2023). CMTM6 promotes hepatocellular carcinoma progression through stabilizing beta-catenin. Cancer Lett, 216585. 10.1016/j.canlet.2023.216585.
15. Mohapatra, P., Shriwas, O., Mohanty, S., Ghosh, A., Smita, S., Kaushik, S.R., Arya, R., Rath, R., Das Majumdar, S.K., Muduly, D.K., et al. (2021). CMTM6 drives cisplatin resistance by regulating Wnt signaling through the ENO-1/AKT/GSK3beta axis. JCI Insight *6*, e143643. 10.1172/jci.insight.143643.
16. Burr, M.L., Sparbier, C.E., Chan, Y.C., Williamson, J.C., Woods, K., Beavis, P.A., Lam, E.Y.N., Henderson, M.A., Bell, C.C., Stolzenburg, S., et al. (2017). CMTM6 maintains the expression of PD-L1 and regulates anti-tumour immunity. Nature *549*, 101-105. 10.1038/nature23643.
17. Mezzadra, R., Sun, C., Jae, L.T., Gomez-Eerland, R., de Vries, E., Wu, W., Logtenberg, M.E.W., Slagter, M., Rozeman, E.A., Hofland, I., et al. (2017). Identification of CMTM6 and CMTM4 as PD-L1 protein regulators. Nature *549*, 106-110. 10.1038/nature23669.
18. Ho, P., Melms, J.C., Rogava, M., Frangieh, C.J., Pozniak, J., Shah, S.B., Walsh, Z., Kyrysyuk, O., Amin, A.D., Caprio, L., et al. (2023). The CD58-CD2 axis is co-regulated with PD-L1 via CMTM6 and shapes anti-tumor immunity. Cancer Cell *41*, 1207-1221 e1212. 10.1016/j.ccell.2023.05.014.
19. Miao, B., Hu, Z., Mezzadra, R., Hoeijmakers, L., Fauster, A., Du, S., Yang, Z., Sator-Schmitt, M., Engel, H., Li, X., et al. (2023). CMTM6 shapes antitumor T cell response through modulating protein expression of CD58 and PD-L1. Cancer Cell *41*, 1817-1828 e1819. 10.1016/j.ccell.2023.08.008.
20. Jia, X.M., Long, Y.R., Yu, X.L., Chen, R.Q., Gong, L.K., and Geng, Y. (2022). Construction of stable membranal CMTM6-PD-L1 full-length complex to evaluate the PD-1/PD-L1-CMTM6 interaction and develop anti-tumor anti-CMTM6 nanobody. Acta Pharmacol. Sin. *44*, 1095–1104. 10.1038/s41401-022-01020-3.
21. Long, Y., Chen, R., Yu, X., Tong, Y., Peng, X., Li, F., Hu, C., Sun, J., and Gong, L. (2023). Suppression of tumor or host intrinsic CMTM6 drives antitumor cytotoxicity in a PD-L1-independent manner. Cancer Immunol Res *11*, 241-260. 10.1158/2326-6066.CIR-22-0439.
22. Qin, Z., Richter, G., Schüler, T., Ibe, S., Cao, X., and Blankenstein, T. (1998). B cells inhibit induction of T cell-dependent tumor immunity. Nat. Med. *4*, 627-630. 10.1038/nm0598-627.
23. Perricone, M.A., Smith, K.A., Claussen, K.A., Plog, M.S., Hempel, D.M., Roberts, B.L., St George, J.A., and Kaplan, J.M. (2004). Enhanced efficacy of melanoma vaccines in the absence of B lymphocytes. J. Immunother. *27*, 273-281. 10.1097/00002371-200407000-00003.
24. Mizoguchi, A., Mizoguchi, E., Takedatsu, H., Blumberg, R.S., and Bhan, A.K. (2002). Chronic intestinal inflammatory condition generates IL-10-producing regulatory B cell subset characterized by CD1d upregulation. Immunity *16*, 219-230. 10.1016/s1074-7613(02)00274-1.
25. Pylayeva-Gupta, Y., Das, S., Handler, J.S., Hajdu, C.H., Coffre, M., Koralov, S.B., and Bar-Sagi, D. (2016). IL35-Producing B Cells Promote the Development of Pancreatic Neoplasia. Cancer Discov. *6*, 247-255. 10.1158/2159-8290.CD-15-0843.
26. Takahashi, R., Macchini, M., Sunagawa, M., Jiang, Z., Tanaka, T., Valenti, G., Renz, B.W., White, R.A., Hayakawa, Y., Westphalen, C.B., et al. (2021). Interleukin-1β-induced pancreatitis promotes pancreatic ductal adenocarcinoma via B lymphocyte-mediated immune suppression. Gut *70*, 330-341. 10.1136/gutjnl-2019-319912.

27. Xiao, X., Lao, X.M., Chen, M.M., Liu, R.X., Wei, Y., Ouyang, F.Z., Chen, D.P., Zhao, X.Y., Zhao, Q., Li, X.F., et al. (2016). PD-1hi Identifies a Novel Regulatory B-cell Population in Human Hepatoma That Promotes Disease Progression. Cancer Discov. *6*, 546-559. 10.1158/2159-8290.CD-15-1408.
28. Shalapour, S., Lin, X.J., Bastian, I.N., Brain, J., Burt, A.D., Aksenov, A.A., Vrbanac, A.F., Li, W., Perkins, A., Matsutani, T., et al. (2017). Inflammation-induced IgA+ cells dismantle anti-liver cancer immunity. Nature *551*, 340-345. 10.1038/nature24302.
29. Biswas, S., Mandal, G., Payne, K.K., Anadon, C.M., Gatenbee, C.D., Chaurio, R.A., Costich, T.L., Moran, C., Harro, C.M., Rigolizzo, K.E., et al. (2021). IgA transcytosis and antigen recognition govern ovarian cancer immunity. Nature *591*, 464-470. 10.1038/s41586-020-03144-0.
30. Tang, T., Cheng, X., Truong, B., Sun, L., Yang, X., and Wang, H. (2021). Molecular basis and therapeutic implications of CD40/CD40L immune checkpoint. Pharmacol. Ther. *219*, 107709. 10.1016/j.pharmthera.2020.107709.
31. Xu, J., Foy, T.M., Laman, J.D., Elliott, E.A., Dunn, J.J., Waldschmidt, T.J., Elsemore, J., Noelle, R.J., and Flavell, R.A. (1994). Mice deficient for the CD40 ligand. Immunity *1*, 423-431. 10.1016/1074-7613(94)90073-6.
32. Bergqvist, P., Gardby, E., Stensson, A., Bemark, M., and Lycke, N.Y. (2006). Gut IgA class switch recombination in the absence of CD40 does not occur in the lamina propria and is independent of germinal centers. J Immunol *177*, 7772-7783. 10.4049/jimmunol.177.11.7772.
33. Chen, Y., Yu, M., Zheng, Y., Fu, G., Xin, G., Zhu, W., Luo, L., Burns, R., Li, Q.Z., Dent, A.L., et al. (2019). CXCR5(+)PD-1(+) follicular helper CD8 T cells control B cell tolerance. Nat Commun *10*, 4415. 10.1038/s41467-019-12446-5.
34. Koike, T., Harada, K., Horiuchi, S., and Kitamura, D. (2019). The quantity of CD40 signaling determines the differentiation of B cells into functionally distinct memory cell subsets. Elife *8*. 10.7554/eLife.44245.
35. Xing, F., Gao, H., Chen, G., Sun, L., Sun, J., Qiao, X., Xue, J., and Liu, C. (2023). CMTM6 overexpression confers trastuzumab resistance in HER2-positive breast cancer. Mol Cancer *22*, 6. 10.1186/s12943-023-01716-y.

STAR*METHODS

KEY RESOURCES TABLE

REAGENT or RESOURCE	SOURCE	IDENTIFIER
Antibodies		
Ms CD45R/B220 PerCP-Cy5.5 RA3-6B2	BD Bioscience	Cat# 552771
BV650 Rat Anti-Mouse CD45R/B220 (RA3-6B2)	BD Bioscience	Cat# 563893
PE Hamster Anti-Mouse CD27 (LG.3A10)	BD Bioscience	Cat# 558754
PE-Cy7 Hamster Anti-Mouse CD27 (LG.3A10)	BD Bioscience	Cat# 563604
Ms IgM BV605 II/41	BD Bioscience	Cat# 743325
APC Rat Anti-Mouse IgD (11-26c.2a)	BD Bioscience	Cat# 560868
FITC Rat Anti-Mouse CD19 (1D3)	BD Bioscience	Cat# 553785
PE-Cy7 Rat Anti-Mouse CD43 (S7)	BD Bioscience	Cat# 562866
Ms CD5 BV510 53-7.3	BD Bioscience	Cat# 563069
MS CD38 BV786 90/CD38	BD Bioscience	Cat# 740887
BV421 Rat Anti-Mouse CD24 (M1/69)	BD Bioscience	Cat# 562563
Ms CD40 BV650 3/23	BD Bioscience	Cat# 740492
PE Rat Anti-Mouse T- and B-Cell Activation Antigen (GL7)	BD Bioscience	Cat# 561530
BV786 Rat Anti-Mouse CD23 (B3B4)	BD Bioscience	Cat# 563988
BV421 Rat Anti-Mouse CD21/CD35 (7G6)	BD Bioscience	Cat# 562756
PE Rat Anti-Mouse CD40(3/23)	BD Bioscience	Cat# 561846
Ms CD4 BV421 GK1.5	BD Bioscience	Cat# 562891
Ms CD8a BV510 53-6.7	BD Bioscience	Cat# 563068
Ms CD3e APC-Cy7 145-2C11	BD Bioscience	Cat# 557596
FITC Rat Anti-Mouse CD45 (30-F11)	BD Bioscience	Cat# 553079
Ms CD86 APC GL1	BD Bioscience	Cat# 558703
PE Hamster Anti-Mouse CD69 (H1.2F3)	BD Bioscience	Cat# 561932
Ms TNF BV650 MP6-XT22	BD Bioscience	Cat# 563943

BV786 Rat Anti-Mouse IFN-γ XMG1.2	BD Bioscience	Cat# 563773
Ms I-A/I-E BV510 2G9	BD Bioscience	Cat# 743871
BV650 Rat Anti-Mouse CD138 (281-2)	BD Bioscience	Cat# 564068
BV510 Hamster Anti-Mouse CD95 (Jo2)	BD Bioscience	Cat# 563646
APC Rat anti-Mouse CD138 (281-2)	BD Bioscience	Cat# 558626
ANTI-MOUSE GRANZYME B (NGZB) PE-CYANINE	eBioscience	Cat# 25-8898-82
ANTI-MO PERFORIN (EBIOOMAK-D) APC	eBioscience	Cat# 17-9392-80
Anti-CMTM6 antibody [EPR23015-45]	Abcam	Cat# ab264067
Goat Anti-Rabbit IgG H&L (Alexa Fluor® 647)	Abcam	Cat# ab150079
Goat Anti-Mouse IgM, F(ab')2 Antibody	CST	Cat# 46315S
InVivoMAb anti-mouse CD20	BioXcell	Cat# BE0356
InVivoMAb anti-mouse CD40	BioXcell	Cat# BE0016-2
Mouse IgG	This lab	N/A
Bacterial and virus strains		
DH5α	Vazyme	Cat# C502-02
Stbl3	Absin	Cat# abs60045
Chemicals, peptides, and recombinant proteins		
Imiquimod	MCE	Cat# HY-B0180
Brefeldin A (BFA) Solution	BD Pharmingen	Cat# 347688
Mouse IL-2	Genscript	Cat# Z02764
Mouse IL-21	MCE	Cat# HY-P700199AF
Mouse BAFF	MCE	Cat# HY-P700161AF
Mouse IL-4	MCE	Cat# HY-P70653
LPS (055:B5)	Merck	Cat# L6529
Agatolimod	MCE	Cat# HY-150218

Critical commercial assays		
Cell Counting Kit (CCK-8)	Yeasen	Cat# 40203ES60
Cytofix/Cytoperm Soln Kit	BD Pharmingen	Cat# 554714
Transcription Factor Buffer Set	BD Pharmingen	Cat# 562574
Phosflow™ Perm Buffer III	BD Pharmingen	Cat# 558050
Cytofix™ Fixation Buffer	BD Pharmingen	Cat# 554655
EasySep™ Mouse Pan-B Cell Isolation Kit	Stemcell	Cat# 19844
Red Blood Cell Lysis Buffer	Yeasen	Cat# 40401ES60
Experimental models: cell lines		
HEK293T	Procell	Cat# CL-0005
CT26	Procell	Cat# CL-0071
B16F10	Procell	Cat# CL-0319
MC38	BNCC	Cat# BNCC337716
Experimental models: organisms/strains		
Mouse: BALB/c	Shanghai Sipp-BK	N/A
Mouse: C57BL/6	Shanghai Sipp-BK	N/A
Mouse: *Cmtm6* KO	GemPharmatech	T013922
Mouse: *Cd274* KO	GemPharmatech	T009724
Mouse: *Cd274&Cmtm6* KO	This lab	N/A
Mouse: *Cd19*-iCre	GemPharmatech	T006948
Mouse: *Cmtm6* flox	GemPharmatech	T013033
Software and algorithms		
Graphpad Prism 8.0 software	GraphPad Software, Inc	http://www.graphpad.com/scientificsoftware/prism/

NovoExpress 1.6.0	Agilent	https://www.agilent.com.cn/zh-cn/product/research-flow-cytometry/flow-cytometry-software
Adobe Illustrator 2017	Adobe	https://www.adobe.com/adobe/illustrator
Discovery studio 2016	BIOVIA	https://www.3ds.com/products/biovia/discovery-studio
Alphafold2-multimer	ColabFold	https://colab.research.google.com/github/sokrypton/ColabFold/blob/main/AlphaFold2.ipynb

RESOURCE AVAILABILITY

Lead contact

Further information and requests for materials should be directed to the Lead Contact: Likun Gong (lkgong@simm.ac.cn).

Materials availability

This study did not generate new unique reagents.

Data and code availability

This study did not generate new codes. Data are all available in the main text or the supplementary materials.

EXPERIMENTAL MODEL AND SUBJECT DETAILS`

Cell lines

CT26, B16F10 and HEK293T cell lines were purchased from Procell. MC38 cell line was purchased from BNCC. B16-F10 and HEK293T cells were cultured in Dulbecco's Modified Eagle Medium (DMEM; Meilunbio) supplemented with 1% penicillin/streptomycin (P/S; Invitrogen) and 10% heat-inactivated fetal bovine serum (FBS; Life Technologies). CT26 and MC38 were cultured in RPMI1640 medium (Meilunbio) containing 1% P/S and 10% FBS. All cells were cultured at 37°C in a 5% CO_2 humidified atmosphere.

Animals

Female (Six-to eight-week-old) BALB/c and C57BL/6 mice were purchased from the Shanghai Slack Animal. *Cmtm6*$^{-/-}$, *Cd274*$^{-/-}$, *Cd19*-iCre and *Cmtm6*^{flox} mice were purchased from GemPharmatech. CMTM6 and PD-L1 double knockout mice were obtained by *Cmtm6*$^{-/-}$ and *Cd274*$^{-/-}$ mice hybridization. The *Cmtm6*^{flox} mice were bred to the *Cd19*-iCre mice to generate *Cmtm6*$^{fl/fl}$ *Cd19*$^{cre+}$ mice. All mice were maintained under specific pathogen-free (SPF) conditions in the animal facility of the Shanghai Institute of Materia Medica, Chinese Academy of Sciences (SIMM). Animal care and experiments were performed in accordance with the protocols approved by the Institutional Laboratory Animal Care and Use Committee (IACUC).

METHOD DETAILS

Primary B cell isolation and culture

WT or *Cmtm6*$^{-/-}$ C57BL/6 mice were sacrificed, and the spleens or lymph nodes were collected for single-cell suspensions. Single-cell suspensions were obtained by grinding tissues through the rubber end of a 2 mL syringe (92311610, Sinopharm) and then were filtered through 70-μm Cell Strainers (WHB-70um, WHB). Single cells were subject to erythrocyte removal by red blood cell lysis buffer (40401ES60, Yeasen).

Highly purified B cells was isolated from splenocytes by immunomagnetic negative selection. The sorting process follows the instructions of the EasySep™ Mouse B Cell Isolation Kit (19854, Stemcell). Briefly, splenocytes were blocked by rat serum. Cells were added with isolation cocktail and incubated for 10 min at room temperature. Then, cells were added with RapidSpheres and incubated for 2.5 min at room temperature. Finally, B cells were sorted out by magnet and washed for subsequent experiments.

Primary B cells were cultured in RPMI1640 medium (Meilunbio) containing 1% P/S, 10% FBS, 50 ng/mL of IL-2 (Z02764, GenScript), 10 ng/mL of IL-4 (HY-P70653, MCE), 10 ng/mL of IL-21 (HY-P700199AF, MCE), and 10 ng/mL of BAFF (HY-P700161AF, MCE).

Activation analysis of primary B cells

1×10^6 of splenocytes or lymph node cells or primary B cells were added to 24-well plates and were stimulated with the TLR4 agonist LPS (L6529, Merck), the TLR7 agonist Imiquimod (HY-B0180, MCE), the TLR9 agonist Agatolimod (HY-150218, MCE), the BCR agonist anti-IgM antibody (46315S, CST), or the CD40 agonist FGK45 antibody (BE0016-2, BioXcell) for 24 h separately for activation phenotype analysis. Dissolution and preparation of agonists were performed following the manufacturer's recommendations. Indicators of activation of primary B cells, CD69, CD86 and MHC II, were detected by flow cytometry.

In vitro proliferation and survival analysis of primary B cells

For the cell proliferation assay, 1×10^5 of primary B cells (100 μL) were seeded in 96-well plates. WT or Cmtm6 KO B cells were added with PBS, 2 μg/mL of CD40 agonist, or 15 μg/mL of CD40 agonist, respectively. 100 μL of CCK8 (40203ES60, Yeasen) was added at 0 h, 36 h, 72 h, respectively, and the signal was read at OD 450 nm by an automatic microplate reader SpectraMax (Molecular Devices).

For the survival assay, 1×10^6 of WT or Cmtm6 KO primary B cells were added to 24-well plates and were stimulated with PBS, 2 μg/mL of CD40 agonist, or 10 μg/mL of CD40 agonist, respectively. After 72 h, B cells were collected and stained with 5 μL of 7-AAD (559925, BD Pharmingen) at room temperature for 10 min. Subsequently, B cells were examined by flow cytometry to determine the proportion of 7-AAD$^+$ dead cells.

In vitro differentiation of germinal center B cells

WT or Cmtm6 KO primary spleen B cells were cultured in RPMI1640 medium containing 1% P/S, 10% FBS, 50 ng/mL of IL-2, 10 ng/mL of IL-4, 10 ng/mL of IL-21, and 10 ng/mL of BAFF to maintain their survival. To induce the differentiation of primary B cells to germinal center B cells, 2 μg/mL or 5 μg/mL of CD40 agonist was added to the medium and incubated for 72 h. CD95$^+$ GL7$^+$ germinal center B cells were quantified by flow cytometry.

Detection of phosphorylated proteins by flow cytometry

2×10^6 of WT or Cmtm6 KO primary spleen B cells were added with 5 μg/mL of CD40 agonist at 37℃ for 15 min. After centrifugation, 100 μL of Cytofix Fixation buffer (554655, BD Pharmingen) was added to the cell pellet to fix the cells at room temperature for 8 min. After centrifugation, 200 μL of Perm Buffer III (558050, BD Pharmingen) was added to the cell pellet for permeabilization at 4℃ for 30 min. After centrifugation, primary antibodies against phosphorylated proteins were added to the cell pellet at room temperature for 45 min. Subsequently, the respective fluorescent secondary antibodies were added at room temperature for 45 min. Finally, the levels of phosphorylated proteins were detected by flow cytometry.

B cell depletion study

Mice were randomly divided and injected with tumor cells (CT26, B16F10 or MC38) subcutaneously, which was defined as day 0. Generally, B cells were deleted by intraperitoneal (i.p.) injection of anti-CD20 (BE0356, BioXcell) on day -2 (150 μg/each) and day 2 (150 μg/each). For the adoptive transfusion of B cells experiments, B cells were deleted by i.p. injection of anti-CD20 on day -12 (150 μg/each) and day -10 (150 μg/each). The deletion effect of CD45$^+$ B220$^+$ B cells in tumors and dLNs was identified by flow cytometry.

In vivo tumor models

For all the subcutaneous models, mice were randomly grouped and injected subcutaneously with 1×10^6 tumor cells (CT26, MC38, B16F10, MC38-OVA or B16-OVA) in the right forelimb. Tumor volume was measured and recorded every two or three days. Tumor volume was calculated as tumor volume (mm^3) = tumor length × width × width/2, and tumor growth curves were plotted. At least four time points after tumor inoculation, the mice were sacrificed and the tumors harvested for weighing, photographing, or other purposes. The euthanasia endpoints were set as tumors larger than 2000 mm^3 or larger than 20 mm in length or mice with significant weight loss.

In vivo treatment studies

Studies of anti-CD40 (BE0016-2, BioXcell) therapy in mice bearing CT26, MC38 and B16F10 tumors are consistent with the descriptions above. The administration methods of each drug are shown in the respective flow charts in the figures.

Immunophenotype analysis

For immunotyping of intratumoral cells, tumor tissues were digested by 1 mg/mL of collagenase IV (40510ES60, Yeasen) and 1 mg/mL of hyaluronidase (20426ES60, Yeasen) and were filtered through 75-micron nylon mesh (7061011, Dakewe) into single cell suspensions and then were subjected to erythrocyte removal by red blood cell lysis buffer (40401ES60, Yeasen). Then the cells were blocked with 4% FBS and anti-CD16/CD32 (553141, BD Biosciences), incubated with surface marker antibodies for 20 minutes at 4℃ and then permeabilized with BD Cytofix/Cytoperm buffer (554714) before intracellular labeling antibodies were added for 30 minutes at 4℃.

For immunotyping of splenocytes and lymph node cells, single-cell suspensions were obtained by grinding tissues through the rubber end of a 2 mL syringe and then were filtered through 75-micron nylon mesh. Single cells were subject to erythrocyte removal by red blood cell lysis buffer. The other staining steps are the same as above.

Flow cytometry analysis was performed using ACEA NovoCyte (Agilent) and data processing was done through NovoExpress software (version 1.6.0). Antibody staining was performed following the manufacturer's recommendations. Please refer to the key resources table for information about the antibodies used.

Adoptive transfusion of B cells

Mice were randomly divided and injected with tumor cells (B16F10 or MC38) subcutaneously, which was defined as day 0. B cells were deleted by i.p. injection of anti-CD20 on day -12 (150 μg/each) and day -10 (150 μg/each). When the tumor volume reached approximately 100 mm^3 (MC38: day 8; B16F10: day 5), 6×10^6 B cells were injected peritumorally. B cells were obtained from spleens of WT mice or *Cmtm6* KO mice by magnetic cell sorting. Tumor growth kinetics, volumes and weights were measured.

Single-cell sequencing data analysis

Single cell RNA-seq data used in this study were all from publicly available data. Data for CMTM6 expression in immune cells were obtained from the GEO database (GSE127465). The SpringViewer interactive tool was used to analyze the data.

RNA-seq

About 30 mg of fresh spleen tissues or 2×10^6 splenic B cells were obtained from sacrificed mice. RNA isolation, transcriptome libraries construction, sequencing and basic data analysis were conducted by BGI. Based on the RNA-seq raw data, differential expression was evaluated with DESeq. A fold-change of 2:1 or greater and a false discovery rate (FDR)-corrected p-value of 0.05 or less were set as the threshold for differential genes.

CMTM6-CD40 interaction analysis

For co-immunoprecipitation experiments, we mainly used Immunoprecipitation Kit with Protein G Magnetic Beads (P2177S, Beyotime). Experiments were performed following the manufacturer's recommendations. Cells were lysed in Lysis Buffer with Protease Inhibitors for 30 min at 4℃. After sufficient lysis, centrifuge the cells at 10,000×g for 5minutes at 4℃ and

take the supernatant. The Protein G magnetic beads were mixed with primary antibody and incubated for 1 h at room temperature. The magnetic bead-antibody was then added to the sample lysate, mixed, and incubated at room temperature for 2 h. After three washes in Lysis Buffer with Protease Inhibitors, samples were eluted in SDS-PAGE Sample Loading Buffer (1X). Finally, the supernatant was used in the Western blot.

Structure prediction of protein complex

Protein amino acid sequences were obtained from the Uniprot database. AlphaFold2 was utilized to predict the structures of human and mouse CMTM6/CD40 complexes, human and mouse CMTM6/PD-L1 complexes, and human CMTM6/CD58 complexes. We used the Alphafold2-multimer algorithm via Google Colab (https://colab.research.google.com/github/sokrypton/ColabFold/blob/main/AlphaFold2.ipynb) to make predictions. Structural presentation of protein complexes and analysis of interaction sites was performed by Discovery studio. The default parameters of each software were used in the calculations.

QUANTIFICATION AND STATISTICAL ANALYSIS

Statistical methods and software

The animal experiments were randomized but the operators were not blinded to allocation during experiments and outcome analysis. Statistical analysis was performed using GraphPad Prism 8 Software. No statistical methods were used to predetermine the sample size. A Student's t test was used for comparison between the two groups. Multiple comparisons were performed using one-way ANOVA followed by Tukey's multiple comparisons test or two-way ANOVA followed by Tukey's multiple comparisons test. Detailed statistical methods and sample sizes in the experiments are described in each figure legend. All statistical tests were two-sided and P-values < 0.05 were considered to be significant. ns not significant; $*p < 0.05$; $**p < 0.01$; $***p < 0.001$.

Figure Legends

Figure 1. CMTM6 regulates B-cell anti-tumor immunity.

(A) Representative spleen photographs and statistical analysis of splenic index (splenic weight * 100% / body weight) in WT and *Cmtm6* KO mice (n = 10).

(B) Representative spleen photographs in WT and *Cmtm6* KO mice bearing MC38-OVA tumor (n = 4) or B16-OVA tumor (n = 5).

(C) RNA-seq analysis of spleen tissues from WT and *Cmtm6* KO mice (n = 3).

(D) RNA-seq analysis of primary splenic B cells from WT and *Cmtm6* KO mice (n = 3).

(E) B16F10 tumor growth and tumor weight in WT and *Cmtm6* KO mice after B cell deletion by anti-CD20 antibody (n = 8).

(F and G) Tumor growth and tumor weight of MC38 tumors (F) or B16F10 tumors (G) in mice with B cell deletion and WT or *Cmtm6* KO B cells infusion (n = 8).

The data are presented as the mean ± SEM. * $p < 0.05$; *** $p < 0.001$; ns not significant by unpaired t test or one-way ANOVA followed by Tukey's multiple comparisons test.

Figure 2. CMTM6 affects B cell differentiation.

(A and B) Representative gating strategy of splenic naïve B cells, non-class-switching memory B cells, and class-switching memory B cells, germinal center B, and statistical analysis in WT or *Cmtm6* KO mice (n = 10).

(C and D) Representative gating strategy of lymph node naïve B cells, non-class-switching memory B cells, and class-switching memory B cells, germinal center B, and statistical analysis in WT or *Cmtm6* KO mice (n = 10).

(E and F) Representative gating strategy of splenic naïve B cells, non-class-switching memory B cells, and class-switching memory B cells, germinal center B, and statistical analysis in *Cmtm6*/*Cd274* double-KO mice and *Cd274* KO mice (n = 10).

The data are presented as the mean ± SEM. * $p < 0.05$; ** $p < 0.01$; *** $p < 0.001$; ns not significant by unpaired t test or two-way ANOVA followed by Tukey's multiple comparisons test.

Figure 3. CMTM6 affects CD40-mediated B cell activation.

(A-C) Statistical analysis of the proportion of $CD86^+$ (A), the proportion of $CD69^+$ (B), and the mean fluorescence intensity (MFI) of MHC II (C) in splenic B cells from WT or *Cmtm6* KO mice after the action of CD40 agonist (n = 8).

(D and E) Activation analysis of sorted splenic B cells from WT or *Cmtm6* KO mice under CD40 agonism. Representative $CD86^+$ population gating strategy and statistical analysis (D; n = 8). Representative histograms and statistical analysis of MHC II expression in B cells (E; n = 8).

(F-H) Statistical analysis of the proportion of $CD69^+$ (F), the proportion of $CD86^+$ (G), and the MFI of MHC II (H) in lymph node B cells from WT or *Cmtm6* KO mice after the action of CD40 agonist (n = 4).

The data are presented as the mean ± SEM. ** $p < 0.01$; *** $p < 0.001$; ns not significant by two-way ANOVA followed by Tukey's multiple comparisons test.

Figure 4. **CMTM6 maintains membrane levels and function of CD40 in B cells.**

(A) Analysis of CD40 membrane levels in splenic B cells from WT or *Cmtm6* KO mice (n = 10).

(B) Analysis of CD40 membrane levels in various subpopulations of splenic B cells from WT or *Cmtm6* KO mice by flow cytometry (n = 8).

(C) Analysis of CD40 membrane levels in various subpopulations of lymph node B cells from WT or *Cmtm6* KO mice by flow cytometry (n = 8).

(D) Analysis of CD40 membrane levels in various subpopulations of splenic B cells from *Cmtm6*/*Cd274* double-KO mice or *Cd274* KO by flow cytometry (n = 8).

(E) Analysis of CD40 membrane levels in splenic B cells from WT or *Cmtm6* KO mice bearing MC38-OVA tumor (n = 4) or B16-OVA tumor (n = 5).

(F and G) Analysis of phosphorylated p65 and p38 levels in splenic B cells from WT or *Cmtm6* KO mice after CD40 agonism by flow cytometry (n = 4).

(H) Analysis of 7-AAD staining of dead splenic B cells from WT or *Cmtm6* KO mice after CD40 agonism for 72 h (n = 4).

(I) Proliferation analysis of splenic B cells from WT or *Cmtm6* KO mice by CCK8 assay after CD40 agonism for 36 h or 72 h (n = 4).

(J) Analysis of differentiation levels of germinal center B cells in splenic B cells from WT or *Cmtm6* KO mice after CD40 agonism for 72 h (n = 5).

The data are presented as the mean ± SEM. * $p < 0.05$; ** $p < 0.01$; *** $p < 0.001$; ns not significant by unpaired t test or one-way/two-way ANOVA followed by Tukey's multiple comparisons test.

Figure 5. **CMTM6 is an interacting molecule of CD40.**

(A) Co-IP analysis of CMTM6/CD40 protein in Raji cell samples.

(B) Co-IP analysis of CMTM6/CD40 protein in mouse splenocyte samples.

(C) AlphaFold2-predicted structures of full-length complexes of human or mouse CMTM6/CD40, CMTM6/CD58, CMTM6/PD-L1.

(D) Key interaction sites predicted by AlphaFold2 for human or mouse CMTM6/CD40, CMTM6/CD58, CMTM6/PD-L1.

Figure 6. **B-cell CMTM6 impacts the antitumor efficacy of CD40 agonists.**

(A) Effect of B-cell deletion on the efficacy of CD40 agonists against CT26 tumors (n = 8).

(B) Effect of B-cell deletion on the efficacy of CD40 agonists against B16F10 tumors (n = 8).

(C) Effect of B-cell deletion on the efficacy of CD40 agonists against MC38 tumors (n = 8).

(D) Comparison of CD40 agonist antitumor efficacy in WT and *Cmtm6* KO mice in the B16F10 tumor model (n = 10).

(E) Comparison of CD40 agonist antitumor efficacy in WT and *Cmtm6* KO mice in the MC38 tumor model (n = 8).

The data are presented as the mean ± SEM. * $p < 0.05$; ** $p < 0.01$; *** $p < 0.001$; ns not significant by one-way ANOVA followed by Tukey's multiple comparisons test.

Figure 1

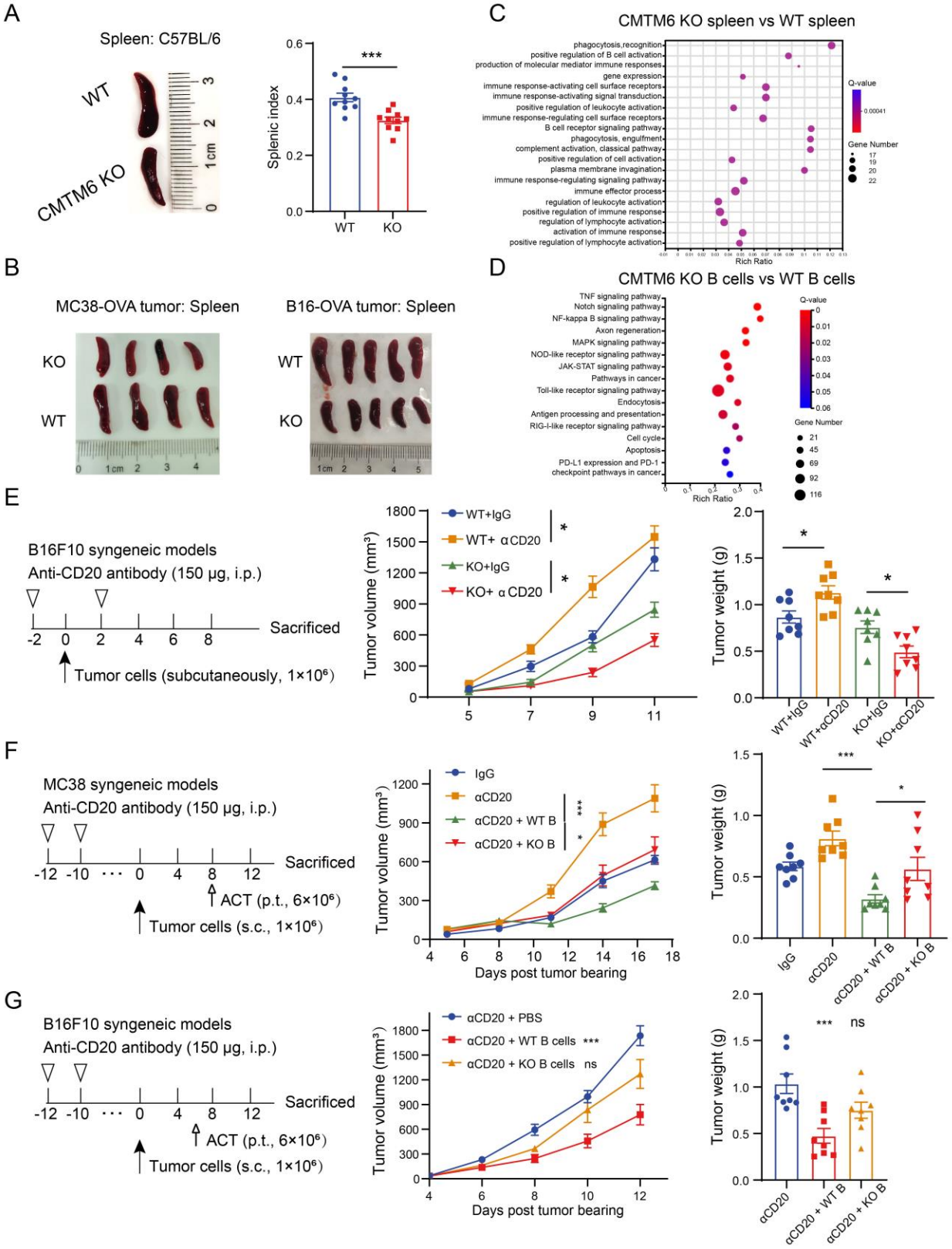
A
Spleen: C57BL/6
WT
CMTM6 KO
Splenic index
***
WT
KO
B
MC38-OVA tumor: Spleen
B16-OVA tumor: Spleen
KO
WT
WT
KO
C
CMTM6 KO spleen vs WT spleen
phagocytosis,recognition
positive regulation of B cell activation
production of molecular mediator immune responses
gene expression
immune response-activating cell surface receptors
immune response-activating signal transduction
positive regulation of leukocyte activation
immune response-regulating cell surface receptors
B cell receptor signaling pathway
phagocytosis, engulfment
complement activation, classical pathway
positive regulation of cell activation
plasma membrane invagination
immune response-regulating signaling pathway
immune effector process
regulation of leukocyte activation
positive regulation of immune response
regulation of lymphocyte activation
activation of immune response
positive regulation of lymphocyte activation
Rich Ratio
Q-value
Gene Number
D
CMTM6 KO B cells vs WT B cells
TNF signaling pathway
Notch signaling pathway
NF-kappa B signaling pathway
Axon regeneration
MAPK signaling pathway
NOD-like receptor signaling pathway
JAK-STAT signaling pathway
Pathways in cancer
Toll-like receptor signaling pathway
Endocytosis
Antigen processing and presentation
RIG-I-like receptor signaling pathway
Cell cycle
Apoptosis
PD-L1 expression and PD-1 checkpoint pathways in cancer
Rich Ratio
Q-value
Gene Number
E
B16F10 syngeneic models
Anti-CD20 antibody (150 μg, i.p.)
Sacrificed
Tumor cells (subcutaneously, 1×10⁶)
WT+IgG
WT+ αCD20
KO+IgG
KO+ αCD20
Tumor volume (mm³)
Tumor weight (g)
WT+IgG
WT+αCD20
KO+IgG
KO+αCD20
F
MC38 syngeneic models
Anti-CD20 antibody (150 μg, i.p.)
Sacrificed
ACT (p.t., 6×10⁶)
Tumor cells (s.c., 1×10⁶)
IgG
αCD20
αCD20 + WT B
αCD20 + KO B
Tumor volume (mm³)
Days post tumor bearing
Tumor weight (g)
IgG
αCD20
αCD20 + WT B
αCD20 + KO B
G
B16F10 syngeneic models
Anti-CD20 antibody (150 μg, i.p.)
Sacrificed
ACT (p.t., 6×10⁶)
Tumor cells (s.c., 1×10⁶)
αCD20 + PBS
αCD20 + WT B cells ***
αCD20 + KO B cells ns
Tumor volume (mm³)
Days post tumor bearing
Tumor weight (g)
ns
αCD20
αCD20 + WT B
αCD20 + KO B

Figure 2

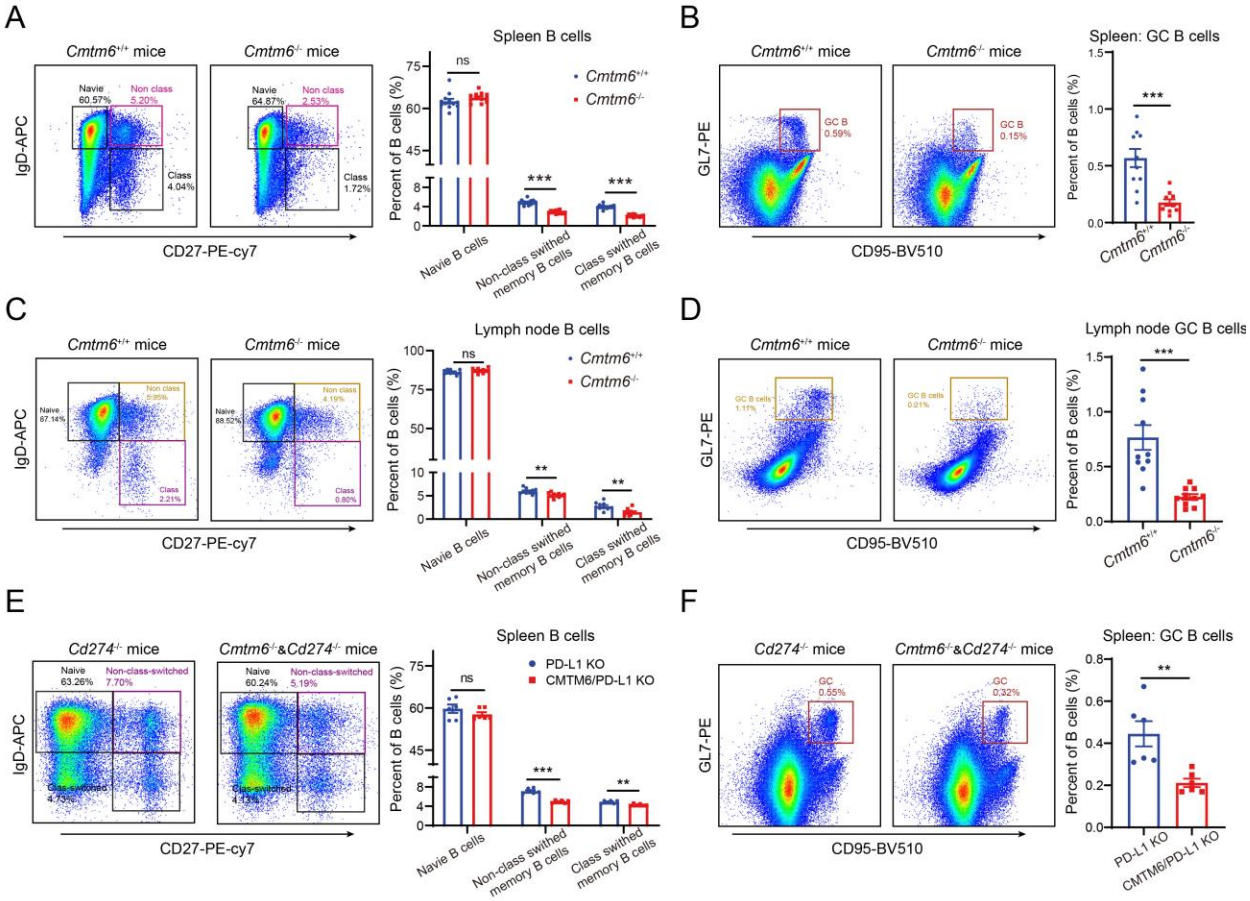
A
Cmtm6+/+ mice
Cmtm6-/- mice
IgD-APC
CD27-PE-cy7
Navie 60.57%
Non class 5.20%
Class 4.04%
Navie 64.67%
Non class 2.53%
Class 1.72%
Spleen B cells
Percent of B cells (%)
ns
***
***
Cmtm6+/+
Cmtm6-/-
Navie B cells
Non-class swithed memory B cells
Class swithed memory B cells
B
Cmtm6+/+ mice
Cmtm6-/- mice
GL7-PE
CD95-BV510
GC B 0.59%
GC B 0.15%
Spleen: GC B cells
Percent of B cells (%)
***
C
Cmtm6+/+ mice
Cmtm6-/- mice
IgD-APC
CD27-PE-cy7
Lymph node B cells
Percent of B cells (%)
ns
**
**
Cmtm6+/+
Cmtm6-/-
Navie B cells
Non-class swithed memory B cells
Class swithed memory B cells
D
Cmtm6+/+ mice
Cmtm6-/- mice
GL7-PE
CD95-BV510
Lymph node GC B cells
Precent of B cells (%)
***
E
Cd274-/- mice
Cmtm6-/-&Cd274-/- mice
IgD-APC
CD27-PE-cy7
Naive 63.26%
Non-class-switched 7.70%
Naive 60.24%
Non-class-switched 5.19%
Spleen B cells
Percent of B cells (%)
ns
***
**
PD-L1 KO
CMTM6/PD-L1 KO
Navie B cells
Non-class swithed memory B cells
Class swithed memory B cells
F
Cd274-/- mice
Cmtm6-/-&Cd274-/- mice
GL7-PE
CD95-BV510
GC 0.55%
GC 0.32%
Spleen: GC B cells
Percent of B cells (%)
**
PD-L1 KO
CMTM6/PD-L1 KO

Figure 3

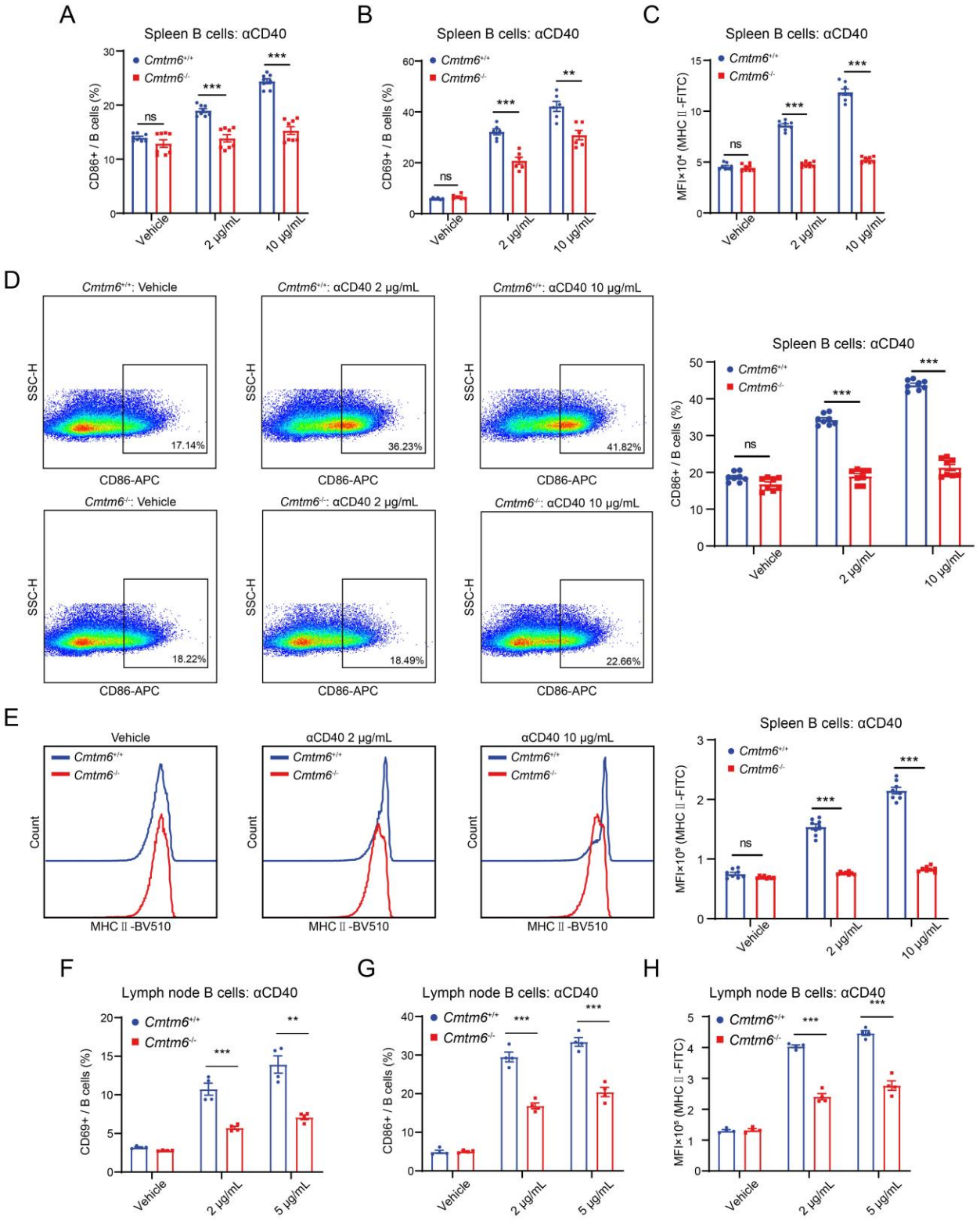
A
Spleen B cells: αCD40
CD86+ / B cells (%)
Cmtm6+/+
Cmtm6-/-
ns
***
Vehicle
2 μg/mL
10 μg/mL
B
Spleen B cells: αCD40
CD69+ / B cells (%)
**
C
Spleen B cells: αCD40
MFI×10⁴ (MHC Ⅱ-FITC)
D
Cmtm6+/+: Vehicle
Cmtm6+/+: αCD40 2 μg/mL
Cmtm6+/+: αCD40 10 μg/mL
Cmtm6-/-: Vehicle
Cmtm6-/-: αCD40 2 μg/mL
Cmtm6-/-: αCD40 10 μg/mL
SSC-H
CD86-APC
17.14%
36.23%
41.82%
18.22%
18.49%
22.66%
E
Vehicle
αCD40 2 μg/mL
αCD40 10 μg/mL
Count
MHC Ⅱ-BV510
MFI×10⁵ (MHC Ⅱ-FITC)
F
Lymph node B cells: αCD40
5 μg/mL
G
H

Figure 4

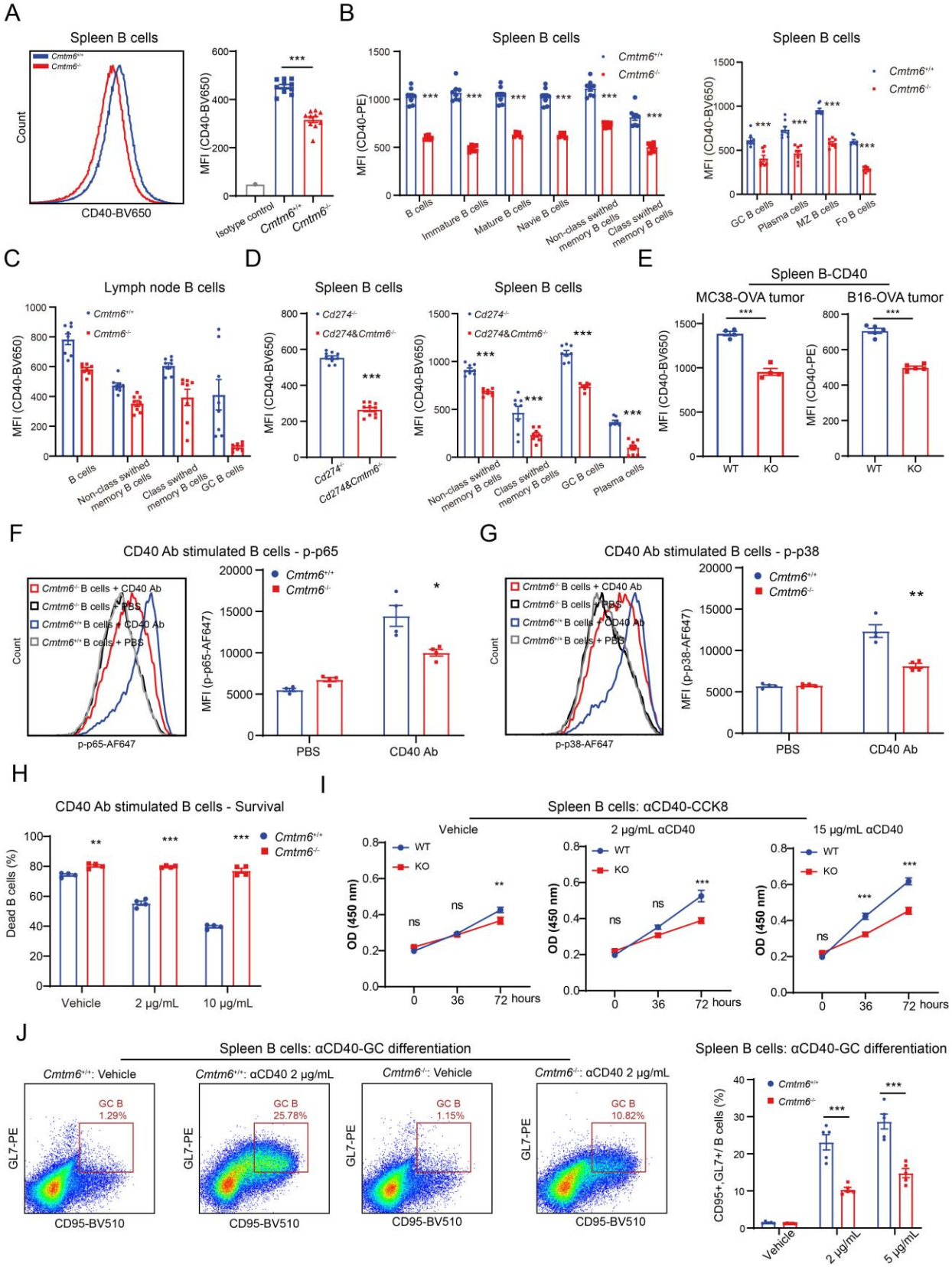
A
Spleen B cells
Count
CD40-BV650
MFI (CD40-BV650)
Isotype control
Cmtm6+/+
Cmtm6-/-
B
Spleen B cells
MFI (CD40-PE)
B cells
Immature B cells
Mature B cells
Navie B cells
Non-class swithed memory B cells
Class swithed memory B cells
GC B cells
Plasma cells
MZ B cells
Fo B cells
C
Lymph node B cells
D
Cd274-/-
Cd274&Cmtm6-/-
E
Spleen B-CD40
MC38-OVA tumor
B16-OVA tumor
WT
KO
F
CD40 Ab stimulated B cells - p-p65
Cmtm6-/- B cells + CD40 Ab
Cmtm6-/- B cells + PBS
Cmtm6+/+ B cells + CD40 Ab
Cmtm6+/+ B cells + PBS
p-p65-AF647
MFI (p-p65-AF647)
PBS
CD40 Ab
G
CD40 Ab stimulated B cells - p-p38
p-p38-AF647
MFI (p-p38-AF647)
H
CD40 Ab stimulated B cells - Survival
Dead B cells (%)
Vehicle
2 μg/mL
10 μg/mL
I
Spleen B cells: αCD40-CCK8
Vehicle
2 μg/mL αCD40
15 μg/mL αCD40
OD (450 nm)
hours
J
Spleen B cells: αCD40-GC differentiation
Cmtm6+/+: Vehicle
Cmtm6+/+: αCD40 2 μg/mL
Cmtm6-/-: Vehicle
Cmtm6-/-: αCD40 2 μg/mL
GC B
1.29%
25.78%
1.15%
10.82%
GL7-PE
CD95-BV510
CD95+,GL7+/ B cells (%)
2 μg/mL
5 μg/mL

Figure 5

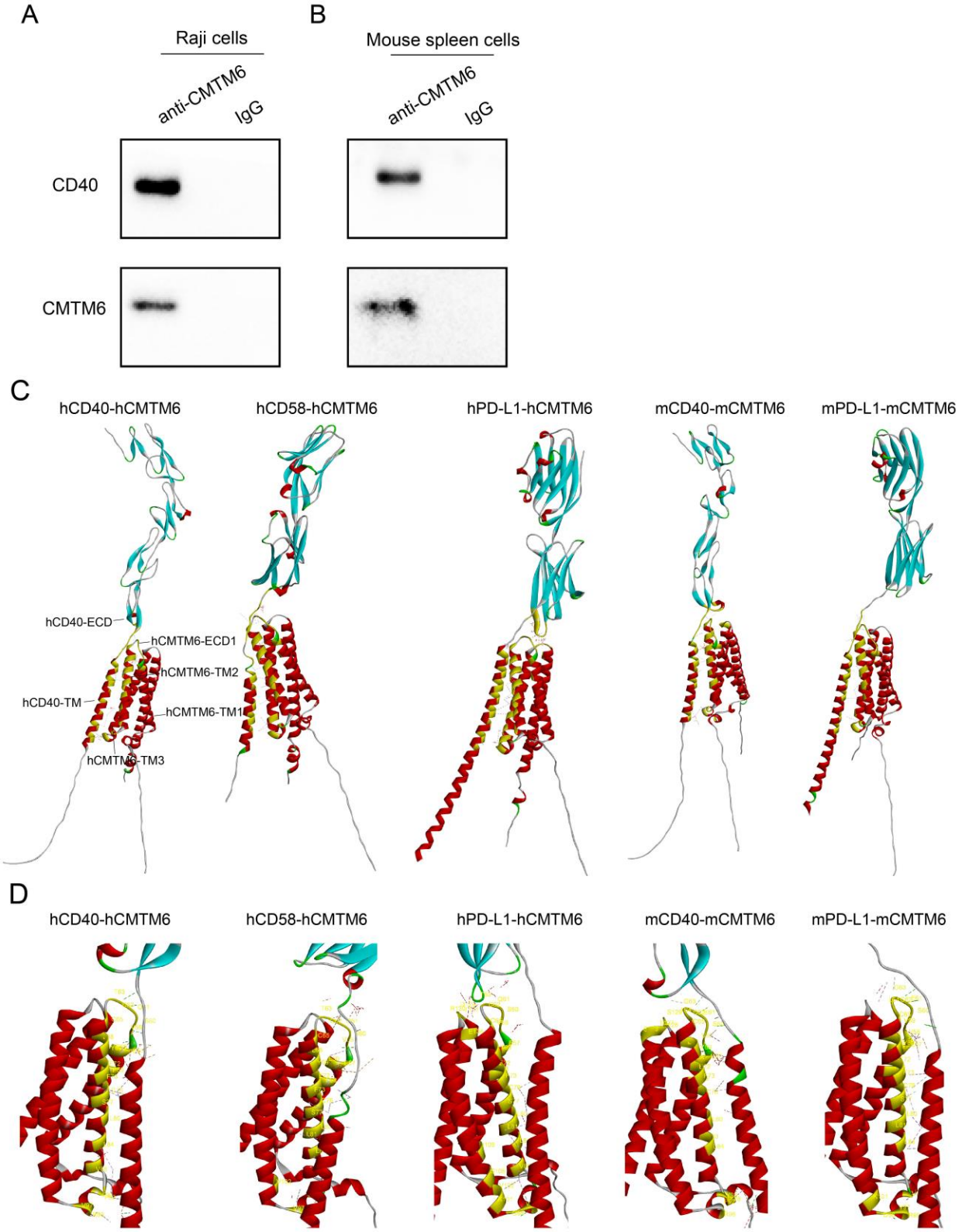
A
Raji cells
anti-CMTM6
IgG
CD40
CMTM6
B
Mouse spleen cells
anti-CMTM6
IgG
C
hCD40-hCMTM6
hCD58-hCMTM6
hPD-L1-hCMTM6
mCD40-mCMTM6
mPD-L1-mCMTM6
hCD40-ECD
hCMTM6-ECD1
hCMTM6-TM2
hCD40-TM
hCMTM6-TM1
hCMTM6-TM3
D
hCD40-hCMTM6
hCD58-hCMTM6
hPD-L1-hCMTM6
mCD40-mCMTM6
mPD-L1-mCMTM6

Figure 6

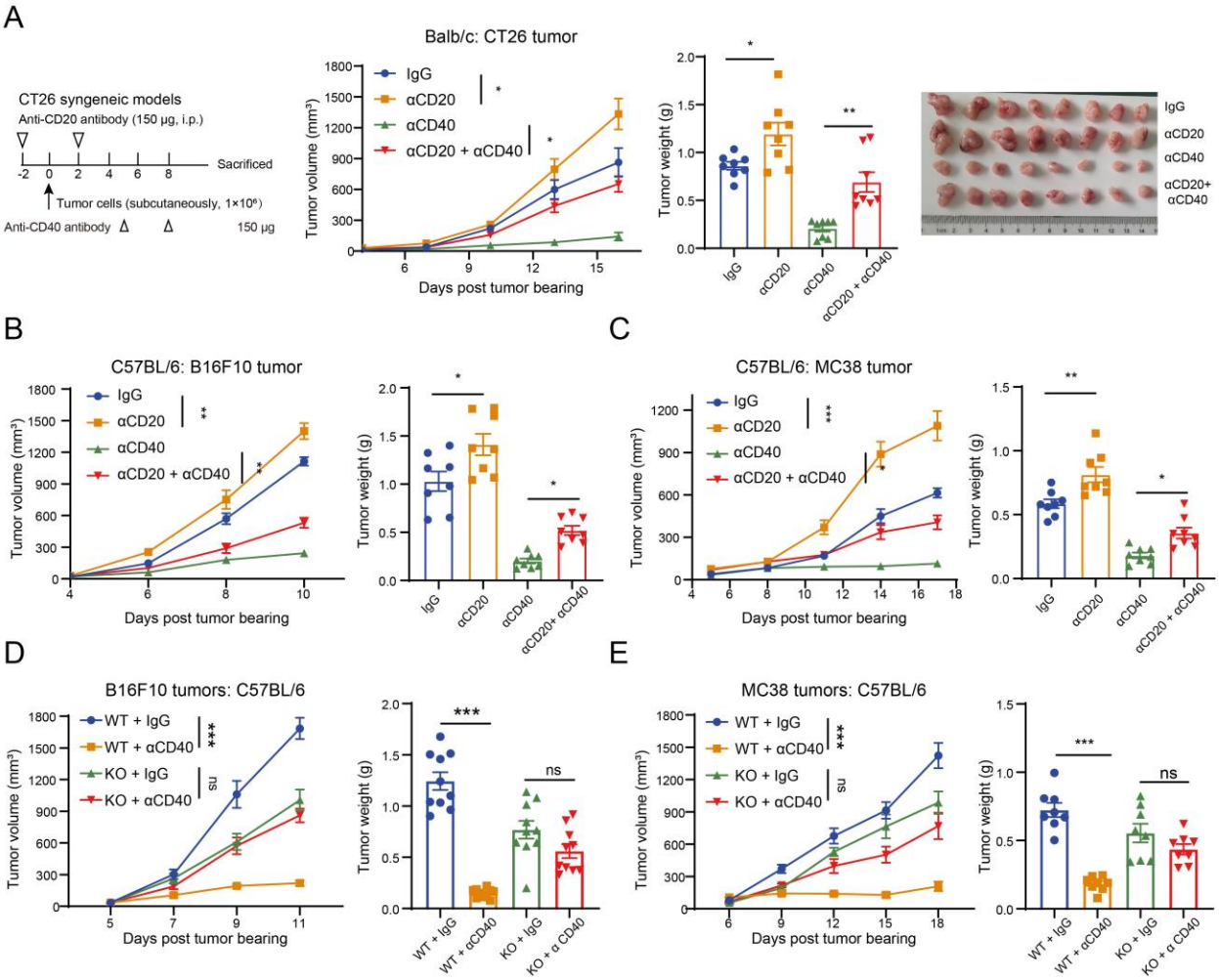
A
CT26 syngeneic models
Anti-CD20 antibody (150 μg, i.p.)
Sacrificed
Tumor cells (subcutaneously, 1×10⁶)
Anti-CD40 antibody
150 μg
Balb/c: CT26 tumor
IgG
αCD20
αCD40
αCD20 + αCD40
Tumor volume (mm³)
Days post tumor bearing
Tumor weight (g)
αCD20+ αCD40
B
C57BL/6: B16F10 tumor
C
C57BL/6: MC38 tumor
D
B16F10 tumors: C57BL/6
WT + IgG
WT + αCD40
KO + IgG
KO + αCD40
ns
E
MC38 tumors: C57BL/6